MRI Sequence Optimization in Head and Neck Imaging and Protocol Design

Start Time: 9/27/2018, 2:40 PM

Author(s)

Kaley Pippin, MD

Fellow

Emory University School of Medicine

Ashley Aiken

Neuroradiology Fellowship Program Director

Emory University School of Medicine

Xin Wu

Assistant Professor of Radiology and Imaging Sciences Neuroradiology Division

Emory University School of Medicine

Abstract Details

Purpose: MRI of the head and neck, particularly the skull base, paranasal sinuses, and larynx, is often critical for diagnosis and treatment planning but presents unique challenges posed by the anatomic complexity, numerous air, soft tissue, and bone interfaces, and potential for patient motion. It is imperative to select appropriate sequences in order to optimize diagnostic performance and scanning time for each anatomic region and indication. The purpose of this project is to outline the application of various MRI sequences available for imaging of the skull base, paranasal sinuses, and larynx and identify factors that may influence sequence choice. Standard sequences will be discussed for each anatomic region, as well as indications for the addition of more advanced sequences. Pearls and pitfalls of each sequence will be explained to assist the radiologist in optimizing protocol design for different clinical applications.

Description: Applicable H&N MRI sequences can be overall grouped into anatomic (T1, T2, fat-suppressed, 3D) and physiologic (DCE, DWI, BOLD) imaging. T1-weighted fast spin echo (FSE), T2-weighted FSE, and fat-suppressed imaging (fat-saturated spin echo, STIR, TIRM) are fast and widely available. Isotropic 3D imaging (CISS/FIESTA, VIBE, SPACE/CUBE/VISTA, Dixon) allows for multiplanar image reconstruction from a single acquisition and can have better spatial resolution than FSE imaging, which are beneficial for delineating the complex anatomy of the head and neck. The available 3D sequences each have their own relative advantages and disadvantages when compared to each other.

Physiologic imaging utilizes contrast enhancement kinetics (DCE), diffusion weighted imaging (DWI), or blood oxygenation level (BOLD) to characterize lesion physiology, particularly useful in predicting chemoradiation response and distinguishing post-therapeutic changes from recurrent tumor. DCE

and BOLD imaging assess tumor blood flow and oxygenation, respectively. Higher tumor vascularity and oxygenation predict a more favorable response to chemoradiation therapy. DCE has been shown to have accuracy of 94.4% in assessing tumor response to radiation therapy, compared to 86% using T1 postcontrast imaging [1]. DWI assesses lesion cellularity with lower ADC values (higher cellularity) often corresponding to malignant lesions.

This presentation will introduce both commonly used MRI sequences in the evaluation of paranasal sinuses, skull base (including temporal bone), and larynx, as well as introduce more advanced sequences which may be tailored for use in the evaluation of specific pathologies and anatomic regions. Important practical factors in protocol design, such as field-of-view and time considerations, will be discussed.

Summary: There are a variety of anatomic and functional MRI sequences useful for H&N imaging, particularly of the skull base, paranasal sinuses, and larynx. Sequences differ in applications to different pathology, spatial resolution, acquisition time, and associated artifacts. It is important for the H&N radiologist to be familiar with these MRI sequences and understand the relative advantages and disadvantages of each sequence in order to optimize imaging protocols for diagnostic accuracy and scan time.

References

1. Baba Y, Furusawa M, Murakami R, et al. Role of dynamic MRI in the evaluation of head and neck cancers treated with radiation therapy. Int J Radiat Oncol Biol Phys 1997;37:7837.

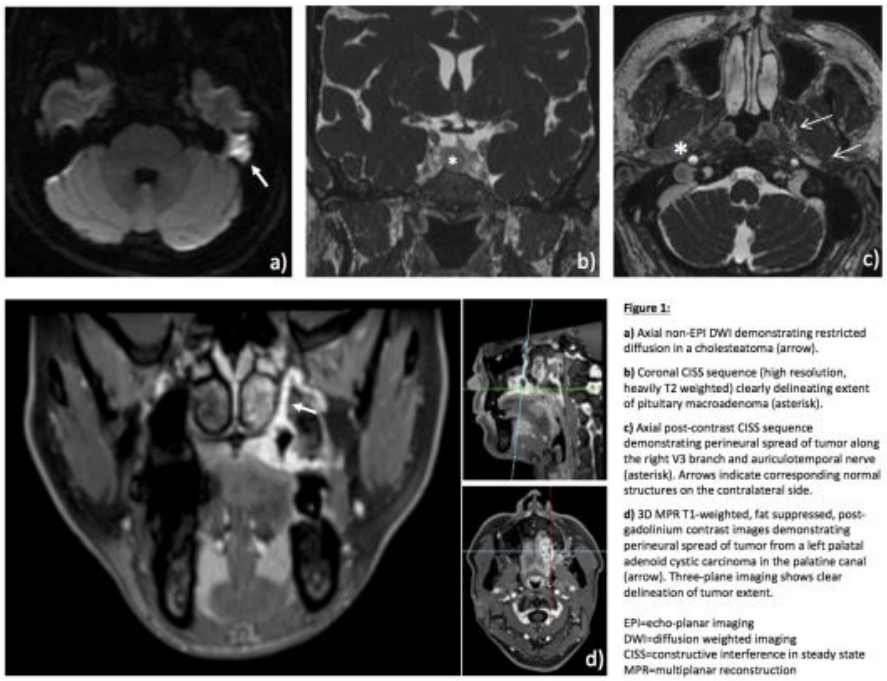

Figure 1:

a) Axial non-EPI DWI demonstrating restricted diffusion in a cholesteatoma (arrow).

b) Coronal CISS sequence (high resolution, heavily T2 weighted) clearly delineating extent of pituitary macroadenoma (asterisk).

c) Axial post-contrast CISS sequence demonstrating perineural spread of tumor along the right V3 branch and auriculotemporal nerve (asterisk). Arrows indicate corresponding normal structures on the contralateral side.

d) 3D MPR T1-weighted, fat suppressed, post-gadolinium contrast images demonstrating perineural spread of tumor from a left palatal adenoid cystic carcinoma in the palatine canal (arrow). Three-plane imaging shows clear delineation of tumor extent.

EPI=echo-planar imaging
DWI=diffusion weighted imaging
CISS=constructive interference in steady state
MPR=multiplanar reconstruction

The value of multiphase MRA in the evaluation of vascular lesions of the head and neck in children. Part 1 technical considerations.

Start Time: 9/27/2018, 2:47 PM

Author(s)
Hervey D. Segall, MD

Professor of Radiology

Medical College/ Children's Hospital of Wisconsin

Jing Qi, MD

Pediatric Neuroradiology

Medical College/ Children's Hospital of Wisconsin

Tejaswini Deshmukh, MD

Pediatric Neuroradiology

Medical College/ Children's Hospital of Wisconsin

Teresa Kelly, MD

Pediatric Neuroradiology

Medical College/ Children's Hospital of Wisconsin

Mohit Maheshwari, MD

Pediatric Neuroradiology

Medical College/ Children's Hospital of Wisconsin

Abstract Details
An institutional review of our experience during the past decade with multiphase MRA in the evaluation of suspect vascular lesions of the head and neck children was performed at the Children's Hospital of Wisconsin.

Our extensive experience resulted from our hypothesis (and eventually, contention) that significant additional information might well be obtained by obtaining serial images after a bolus injection of gadolinium when contrast-enhanced MR was scheduled to be performed in cases of suspected vascular lesions in the head and neck in the pediatric age group. Whenever possible our studies were monitored by a neuroradiologist during the performance of an examination. In each case a scanning zone is selected in order to optimize spatial and temporal resolution. Slices as fast as 1/sec may be obtained following a post tight bolus injection of gadolinium. Subtracted serialograms are easily obtained easily in three orthagonal planes. Although a direct case by case comparison could not be done due to many logistic factors and constraints we found that multiphase MRA added

considerable information when compared to TOF MRA and Doppler ultrasound, etc. Multiphase MRA also proved to be valuable in the follow-up of treated vascular lesions of the head and neck.

We also found that the best examinations (done on several machines from various vendors) were done on our 3T equipment. All MR vendors now offer multiphase MRA techniques that go by a variety of acronyms (GE: TRICKS, Siemens: TWIST, Philips: 4D-TRAK, Hitachi: TRAQ, Toshiba: Freeze Frame). Each vendor's technique is somewhat different but they all share certain similarities, including a 3D spoiled gradient sequence, filling of k-space into at least two categories (central sampling being done at a more rapid/frequent rate than peripheral k-space), interleaving of multiple scan phases to optimize temporal resolution, real time subtraction using a first mask phase and production of multiphase collapsed MIP projections.

The value of multiphase MRA in the evaluation of vascular lesions of the head and neck in children. Part 2 selected clinical experiences.
Start Time: 9/27/2018, 2:54 PM

Author(s)

Hervey D. Segall, MD

Professor of Radiology

Medical College/ Children's Hospital of Wisconsin

Patricia Burrows, MD

Professor of Radiology. Interventional Neuroradiology

Medical College/ Children's Hospital of Wisconsin

Robert Chun, MD

Associate Professor of Otolaryngology

Medical College/Children's Hospital of Wisconsin

Abstract Details
An institutional review of our experience during the past decade with multiphase MRA in the evaluation of suspect vascular lesions of the head and neck children was performed at the Children's Hospital of Wisconsin.

Our extensive experience resulted from our hypothesis (and eventually, contention) that significant additional information might well be obtained by obtaining serial images after a bolus injection of gadolinium when contrast-enhanced MR was scheduled to be performed in cases of suspected vascular lesions in the head and neck in children. This presentation will demonstrate the usefulness of this method in the diagnosis and treatment of a variety of pediatric vascular malformations and lesions within the head and neck in the pediatric age group.

Whereas multiphase MRA is seldom regarded as definitive for intracranial AVMs the method can be definitive for such a lesion in the head and neck as will be shown.

Our pediatric interventionalists have found multiphase MRA to be indispensable in the diagnosis and treatment in fistulous vascular malformation within the neck. In such cases multiphase MRA can enable a correct diagnosis, demonstrate arterial feeders and venous drainage resulting in significant reduction in procedure time, contrast volume and radiation when subsequent conventional angiography and interventional treatment are performed. In fact, the venous drainage may be better demonstrated by multiphase MRA than by conventional angiography.

Multiphase MRA has also proven to be valuable in the follow-up of treated vascular lesions of the

head and neck.

In many cases diagnostic evaluation is initiated by general pediatricians. In cases that might be elusive for a generalist (but more obvious to a specialist dealing with vascular malformations) a convincing diagnosis can be made at the outset with multiphase MRA .

In addition to the above, we will demonstrate cases of hemangiomas, venous malformations and microcystic lymphatic malformations where multiphase MRA was helpful in adding an increment of certainty in diagnosis.

Differentiating PET positive metastatic and reactive lymph nodes in patients with head and neck squamous cell carcinoma using MR texture analysis

Start Time: 9/27/2018, 3:01 PM

Author(s)
Eric K. van Staalduinen, DO
Radiology Resident
Stony Brook University Hospital

Adam Khan, MD
Radiology Resident
Stony Brook University Hospital

Haifang Li, PhD
Imaging Scientist
Stony Brook University Hospital

Kenneth Wengler, MS
Imaging Scientist
Stony Brook University Hospital

Renee F. Cattell, BS
Imaging Scientist
Stony Brook University Hospital

Robert Matthews, MD
Nuclear Medicine
Stony Brook University Hospital

Dinko Franceschi, MD
Nuclear Medicine
Stony Brook University Hospital

Tim Q. Duong, PhD
Imaging Scientist
Stony Brook University Hospital

Lev Bangiyev, DO

Radiology

Stony Brook University Hospital

Abstract Details

Purpose: PET-MRI is a powerful imaging modality in the evaluation of patients with head and neck squamous cell carcinoma. Occasionally the PET findings could be false positive or indeterminate, which may result in unnecessary surgical dissection and radiation therapy. The purpose of our study was to evaluate the use of MR texture features in distinguishing PET positive metastatic and reactive lymph nodes in patients with head and neck squamous cell carcinoma.

Materials and Methods: Following IRB approval, 12 patients with primary head and neck squamous cell carcinoma underwent multiparametric PET-MRI between September 2016 and November 2017. Five patients had neck dissection and were selected for evaluation. PET-MRI studies were compared with pathology reports and lymph nodes were segmented manually from the axial STIR images with 3D ROIs using the texture analysis program LifeX. 37 texture features were extracted for each segmented volume. A t test was used to evaluate for differences between PET positive/Path positive (metastatic) and PET positive/Path negative (reactive) lymph nodes.

Results: Of the 5 patients evaluated, there were 10 path-proven metastatic lymph nodes (SUV 3.9-17.2, mean 8.6 ± 4.2) and 10 path-proven reactive lymph nodes (SUV 2.7-7.3, mean 4.4 ± 1.5). Significant differences were seen in GLCM Entropy log10 ($P = .04$), GLCM Entropy log2 ($P = .04$), GLRLM HGRE ($P = .006$), GLRLM SRHGE ($P = .006$), GLRLM LRHGE ($P = .006$), GLZLM HGZE ($P = .008$), and GLZLM SZHGE ($P = .01$).

Conclusion: There are statistically significant differences in some MR texture features between PET positive metastatic and reactive lymph nodes in patients with head and neck squamous cell carcinoma. MR texture features may be used to help distinguish these lymph nodes in order to guide surgical dissection and radiation therapy.

Diffusion-Weighted Imaging for the Evaluation of the Neck: New Qualitative Assessment Metric with Kappa Analysis
Start Time: 9/27/2018, 3:08 PM

Author(s)

Gloria Guzman, MD, MSc

Assistant Professor of Radiology, Associate Residency Program Director

University of Arizona

Rihan Khan

Associate Professor

University of Arizona

Abstract Details

Purpose:

Current DWI sequences of the head and neck have significant issues with fat saturation, distortion, aliasing/ghosting and resolution that limit their utility, even though the Quantitative Imaging Biomarkers Alliance [QIBA, 2015] has attempted to address these shortcomings through optimized image parameters. We propose to create a standardized method to evaluate neck DWI sequence artifacts that includes qualitative measurements.

Materials and Methods:

A total of 25/37 consecutive suprahyoid or full neck MRIs performed in October 2015 were blindly evaluated by 2 expert neuroradiologists for artifacts using our proposed qualitative artifact scale, which rated them from 1 (no artifact) to 4 (severe artifact) for aliasing/ghosting, geometric distortion, fat saturation quality, and motion. 12 were excluded due to lack of DWI images. The grading scales and imaging examples are seen on Figure 1. Agreement between the two neuroradiologists was quantified using the weighted kappa coefficient (SAS v9.4, Cary, NC).

Results:

The weighted kappa coefficient (95% CI, p-value) for aliasing artifacts was 0.3377 (0.0557-0.6198, p=0.0168), for geometric distortion was 0.0683 (-0.1694-0.3061, p=0.4958), for fat saturation was 0.3119 (0.1608-0.4629, p<0.0001). None of the neuroradiologists noted motion artifacts.

Conclusion:

This preliminary study demonstrated the capability of a new qualitative method to qualitatively assess artifacts in diffusion MRI sequences in neck imaging. Although our preliminary data suggest that portions of this scale are a promising technique to accurately measure artifacts, larger studies with quantitative parameters of geometric distortion, ghosting and residual fat signal.

References:

Chen NK, Guidon A, Chang HC, Song AW. A robust multi-shot scan strategy for high-resolution diffusion weighted MRI enabled by multiplexed sensitivity-encoding (MUSE). Neuroimage 2013; 15(72):41-47.
Chen N.K, Wyrwicz AM. Correction for EPI distortions using multi-echo gradient-echo imaging. Magnetic resonance in medicine 1999; 41(6): 1206-1213.
Quantitative Imaging Biomarker Alliance (QIBA). Perfusion, Diffusion and FlowMRI Biomarker Committee, DWI profile. February 4, 2015. http://qibawiki.rsna.org/index.php/ Perfusion,_Diffusion _and_Flow-MRI_Biomarker_Ctte.

ALIASING / GHOSTING ARTIFACTS	
Score	Description
1	No artifacts
2	Aliasing present but no overlap and no single ghosting ring
3	Aliasing with rim overlap over face, neck / upper chest or single minimally displaced ghosting ring
4	Aliasing significant overlap over neck / upper chest or multiple ghosting rings

GEOMETRIC DISTORTION ARTIFACTS	
Score	Description*
1	No artifacts
2	Distortion limited to 1 quadrant, in area of interest
3	Distortion limited to any 2 quadrants, in area of interest
4	Distortion in any 3 or 4 quadrants, non-diagnostic in area of interest

* The four quadrants are defined by the midline plane separating the left and right side, and by a transverse plane through the mid portion of the spinal canal.

FAT SATURATION QUALITY	
Score	Description
1	Near perfect/perfect
2	Mild impairment - ventral or dorsal fat saturation failure about the level of the chin or at the base of neck
3	Moderate impairment - ventral or dorsal fat saturation failure about the level of the chin & at the base of neck
4	Severe impairment - Ventral & dorsal fat saturation failure at both the level of the chin & at the base of neck

MOTION ARTIFACTS	
Score	Description
1	No artifacts
2	Mild artifacts, not likely to obscure a lesion
3	Moderate artifacts, may obscure a lesion
4	Severe artifacts, non-diagnostic images

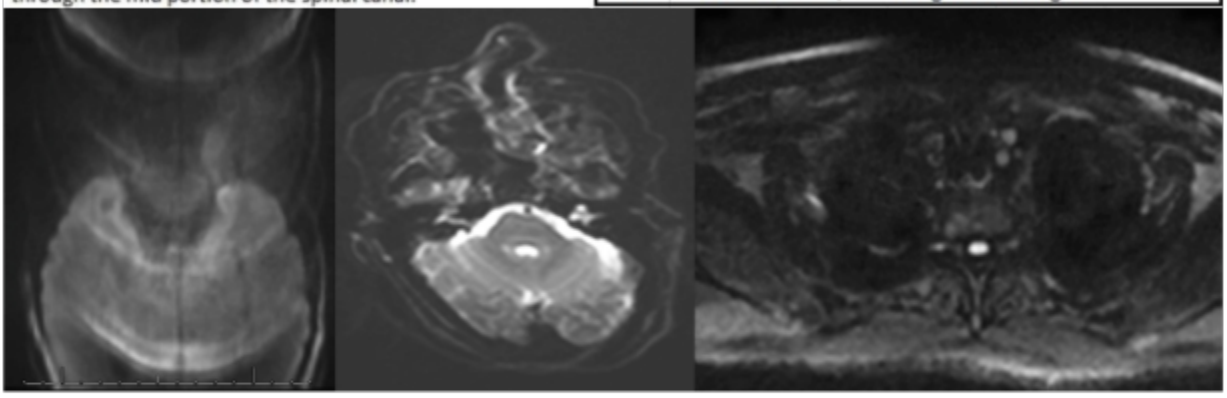

Figure 1: DWI images from three different patients with clinical suspicion of malignancy. A (left), Severe aliasing/ghosting artifact in large portions of the neck, Grade 4. B (center), Severe geometric distortion in 3 or 4 quadrants, Grade 4. C (right), Severe failure of fat saturation in the ventral and dorsal aspect of the neck, Grade 4.

Utility of Diffusion Weighted Imaging for Differentiation of Nasopharyngeal Carcinoma, Lymphoma, and Reactive Lymphoid Hyperplasia: a Retrospective Review
Start Time: 9/27/2018, 3:15 PM

Author(s)

Nathan T. Mortensen, DO

Neuroradiology Fellow

Indiana University School of Medicine

Carrie Norris, MD

Radiology Resident

Indiana University School of Medicine

Kristine Mosier, DMD, PhD

Associate Professor of Radiology and Imaging Sciences

Indiana University School of Medicine

Nicholas A. Koontz, MD

Director of Fellowship Programs, Dean D.T. Maglinte Scholar in Radiology Education, Assistant Professor of Radiology

Indiana University School of Medicine

Abstract Details
Purpose:

The purpose of this study was to evaluate the utility of diffusion weighted imaging (DWI) for differentiating malignancy from reactive lymphoid hyperplasia within the nasopharynx.

Materials & Methods:

In this IRB approved, HIPPAA compliant retrospective review of 18 total patients with histologically proven nasopharyngeal carcinoma, lymphoma, or reactive lymphoid hyperplasia, patients were imaged with 1.5 or 3 T MRI, including DWI. On the ADC map, a free hand region of interest (ROI) was drawn within the lesion to determine the mean ADC value. Similarly, an ROI within the medulla was drawn for an internal control. ROI placement was confirmed by consensus of the principal investigator and senior coauthor. To account for variation in ADC values between scanners, magnetic field strengths (which can lower ADC values as magnetic field strength increases), and matrix sizes, a normalized ADC ratio was constructed by dividing the mean ADC value of the lesion by the mean ADC value of the medulla (ADC ratio = ADClesion / ADCmedulla). A total of 11

nasopharyngeal carcinomas (NPC), 2 nasopharyngeal lymphomas, and 5 nasopharyngeal adenoid hypertrophy cases were evaluated. Statistical analysis was performed, including parametric and non-parametric test statistics.

Results:

100% (n = 11 of 11) of NPCs demonstrated a lesion-to-medulla ratio < 1.0 with 72% (n = 8 of 11) demonstrating a ratio < 0.9. With respect to lymphoma, 100% (n = 2 of 2) demonstrated a lesion-to-medulla ratio < 1.0, and 50% (n = 1 of 2) demonstrated a ratio approaching 0.5. Lastly, 60% (n = 3 of 5) of reactive lymphoid hyperplasia cases demonstrated a ratio > 1, and 100% (n = 5 of 5) showed a ratio 0.9. There was a statistically significant difference in mean ADC ratio between malignant and benign lesions with both parametric ($p = 0.02$, one-tailed test with unequal variance) and non-parametric ($p < 0.002$) calculation. Excluding lymphoma, there was a statistically significant difference in mean ADC ratio between NPC alone and benign lesions with both parametric ($p = 0.03$, one-tailed test with unequal variance) and non-parametric ($p < 0.004$) calculation. Using a lesion-to-medulla ratio cut point of 0.9, whereby 0.9 or less favors malignancy and > 0.9 favors benignity, we calculated a sensitivity of 84.6%, specificity of 80%, Positive Predictive value of 91.7%, and a Negative Predictive Value of 66.7%.

Conclusion:

DWI may be useful in differentiating benign from malignant lesions in the nasopharynx, as lower ADC ratios were observed in malignant lesions and higher ADC ratios observed in benign lesions.

References:

1. Koontz NA, Wiggins RH. Differentiation of benign and malignant head and neck lesions with diffusion tensor imaging and DWI. AJR 2017; 208:1110-1115

2. Ichikawa Y, et al. Efficacy of diffusion-weighted imaging for the differentiation between lymphomas and carcinomas of the nasopharynx and oropharynx: correlations of apparent diffusion coefficients and histologic features. AJNR 2012;33:761-766

3. Maeda M, et al. Usefulness of the Apparent Diffusion Coefficient in Line Scan Diffusion-Weighted Imaging for Distinguishing between Squamous Cell Carcinomas and Malignant Lymphomas of the Head and Neck. AJNR 2005;26:1186-1192

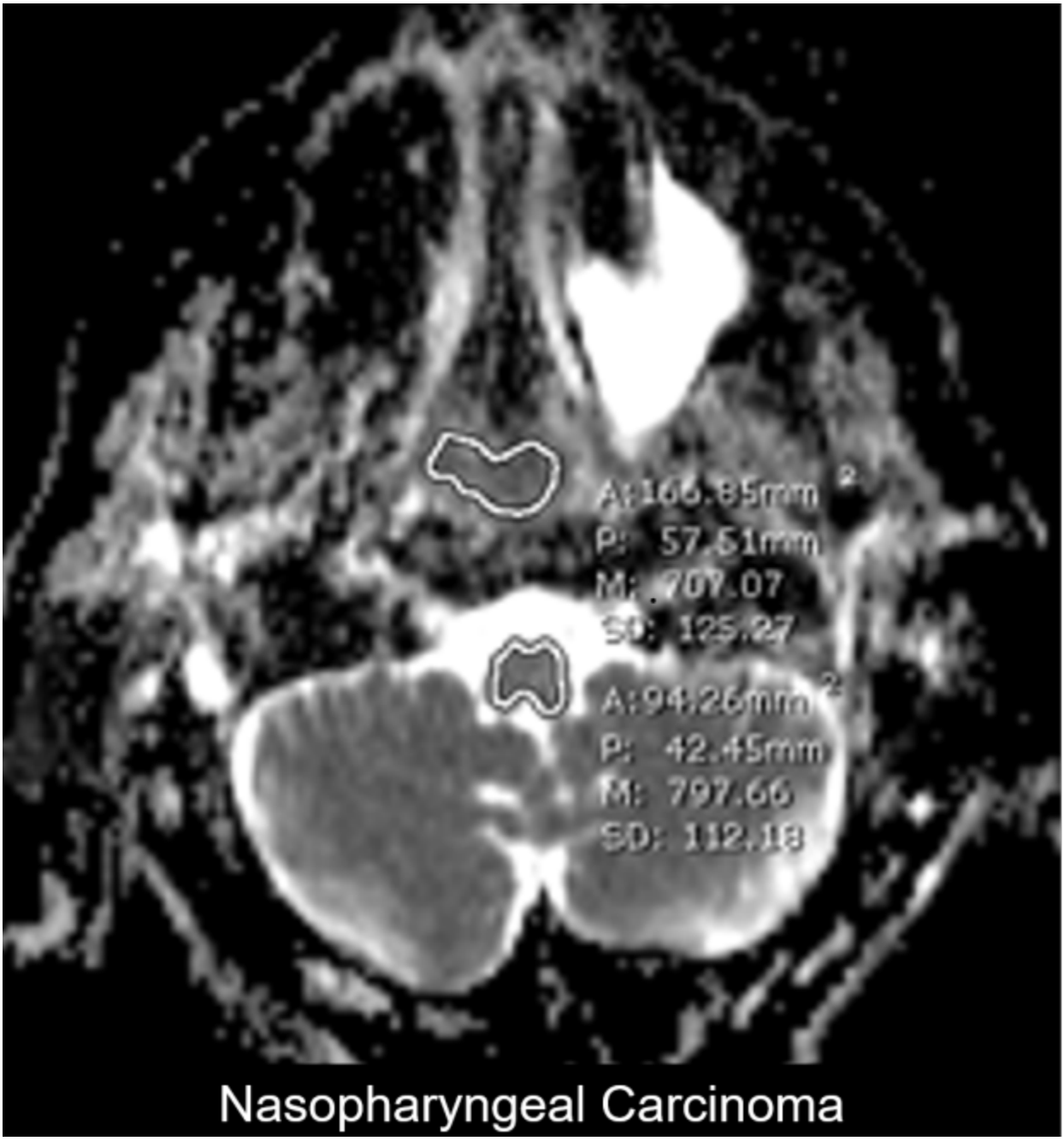

Nasopharyngeal Carcinoma

Multimodal Measures of Perineural Tumor Spread: Does PET FDG correlate with MR Diffusion Anisotropy?

Start Time: 9/27/2018, 3:22 PM

Author(s)
Katie S. Traylor, DO
Neuroradiology Fellow
Indiana University School of Medicine

Nicholas A. Koontz, MD
Director of Fellowship Programs, Dean D.T. Maglinte Scholar in Radiology Education, Assistant Professor of Radiology
Indiana University School of Medicine

Vasantha D. Aaron, MD
Assistant Professor of Clinical Radiology and Imaging Sciences
Indiana University School of Medicine

Justin B. Sims, MD
Assistant Professor of Clinical Radiology and Imaging Services
Indiana University School of Medicine

Kristine Mosier, DMD, PhD
Associate Professor of Radiology and Imaging Sciences
Indiana University School of Medicine

Abstract Details
Introduction: Perineural spread is defined as spread of tumor along named cranial nerves and although estimates vary, is reported to occur in approximately 15-40% of head and neck cancers. Perineural spread is important to identify as the presence of perineural spread significantly decreases overall survival. Previous studies have shown that interactions between glial cell derived neurotrophic factor (GDNF) from nerves and chemokines from adjacent tumor draws the tumor onto the nerve. This process is dependent on glucose utilization. These interactions suggest that a combination of FDG avidity and diffusion imaging measures may improve the sensitivity and specificity of perineural spread. However, the relationship between FDG uptake and diffusion measures including the apparent diffusion coefficient (ADC) and fractional anisotropy (FA) in perineural spread remains unclear.

Purpose: To determine the relationship between the apparent diffusion coefficient (ADC), fractional anisotropy (FA), and standardized uptake value in perineural tumor spread

Materials/Methods: We conducted a retrospective review of patients in our institutional database from 2010-2018. Inclusion criteria included patients with proven or suspected perineural spread with

MRI and PET-MRI or PET-CT exams. A total of 12 patients met inclusion criteria. ROI analysis was performed on the involved nerve as well as the contralateral uninvolved nerve and the brainstem as controls for the ADC and FA measurements. Standard uptake values (SUV) were obtained from the co-registered PET and MR images of the involved nerve. Statistical analysis was performed using ANOVA and non-linear Poisson regression methods accounting for small sample size and ROI volume.

Results:
Perineural spread was identified primarily along V2 and V3 branches of the trigeminal (n = 11) as well as the V1 branch of CN 5 (n = 1). Pathology included squamous cell carcinoma (n = 6), adenoid cystic carcinoma (n = 1), poorly differentiated salivary carcinoma (n = 1), sinonasal small cell carcinoma (n =1), neuroblastoma (n=1), and rhadomyosarcoma (n = 1). All involved nerves (n=12) demonstrated enlargement and enhancement on post-contrast MRI.
There was a statistically significant effect of the SUV on FA, as well as ADC ($p=0.01$). Further, our preliminary data suggests that as the SUV increases, the FA also increases. These results suggests that a higher metabolic activity may be associated with formation of directional structure.

Conclusion:
The results of this study show a relationship between the FA and SUV in perineural spread and suggest that increased FDG uptake is associated higher FA values. This may reflect anisotropy secondary to directional vector of tumor spread along the nerve, or alternatively may represent the signature of neural-tumor tracking.

Greater Occipital Nerve: Radiological anatomy demonstrated by two cases of Tumour Perineural Spread

Start Time: 9/27/2018, 3:29 PM

Author(s)
Maciej Debowski, MBBS
PET PHO
Royal Brisbane and Women's Hospital

Jennifer Sommerville, FRANZCR, MBBS, BPhty
Radiologist
Royal Brisbane and Women's Hospital, University of Queensland

Mitesh Gandhi, FRANZCR
Radiologist
Princess Alexandra Hospital and Queensland X-Ray

Abstract Details

Background: The greater occipital nerve (GON) is a tortuous superficial cutaneous nerve supplying sensory innervation to the posterior scalp. Perineural spread (PNS) is an established form of local invasion but is rarely seen along the GON.
Methods: We present two cases of PNS along the GON which underwent MRI and extensive resection.
Results: A selection of annotated MR images and a diagram is used to illustrate anatomy of the GON which is relevant to the surgeon and radiologist.
Conclusion: This is the first radiological portrayal of the course of perineural tumour spread of the GON as demonstrated on MRI.